A stochastic rainfall model that can reproduce important rainfall properties across the timescales from several minutes to a decade

Dongkyun Kim[1*] and Christian Onof[2]

1. Department of Civil Engineering, Hongik University, Seoul, Korea

2. Department of Civil and Environmental Engineering, Imperial College London, UK

* Corresponding Author: kim.dongkyun@hongik.ac.kr

Abstract

A stochastic rainfall model that can reproduce various rainfall characteristics at timescales between 5 minutes and one decade is introduced. The model generates the fine-scale rainfall time series using a randomized Bartlett-Lewis rectangular pulse model. Then the rainstorms are shuffled such that the correlation structure between the consecutive storms are preserved. Finally, the time series is rearranged again at the monthly timescale based on the result of the separate coarse-scale monthly rainfall model. The method was tested using the 69 years of 5-minute rainfall data recorded at Bochum, Germany. The mean, variance, covariance, skewness, and rainfall intermittency were well reproduced at the timescales from 5 minutes to a decade without any systematic bias. The extreme values were also well reproduced at timescales from 5 minutes to 3 days. The past-7-day rainfall before an extreme rainfall event, which is highly associated with the extreme flow discharge was reproduced well too. The rainstorm shuffling approaches introduced here may be adopted as a standard procedure in combination with any Poisson cluster rainfall model. The methods are simple and parsimonious, yet significantly reduce the systematic underestimation of rainfall variance at coarse scales, and improve the reproduction of skewness, and extreme rainfall depths values at a range of time-scales, thereby addressing well-known shortcomings of Poisson cluster rainfall models.

Keywords: Poisson cluster rainfall model; rainfall variability; timescale; holistic approach

***Highlights (3 to 5 bullet points (maximum 85 characters including spaces per bullet point)**

Highlights

- A novel stochastic rainfall model based on Poisson cluster model was invented.
- The model shuffles generated rainstorms to account for short-term rainfall memory.
- The model shuffles monthly rainfall to account for long-term rainfall memory
- The model accurately reproduces observed rainfall properties from 5min to 10yr timescale.
- Due to this strength, the model can be used to assess the risks of a variety of disasters.

A stochastic rainfall model that can reproduce important rainfall properties across the timescales from several minutes to a decade

Dongkyun Kim[1*] and Christian Onof[2]

1. Department of Civil Engineering, Hongik University, Seoul, Korea

2. Department of Civil and Environmental Engineering, Imperial College London, UK

* Corresponding Author: kim.dongkyun@hongik.ac.kr

Abstract

A stochastic rainfall model that can reproduce various rainfall characteristics at timescales between 5 minutes and one decade is introduced. The model generates the fine-scale rainfall time series using a randomized Bartlett-Lewis rectangular pulse model. Then the rainstorms are shuffled such that the correlation structure between the consecutive storms are preserved. Finally, the time series is rearranged again at the monthly timescale based on the result of the separate coarse-scale monthly rainfall model. The method was tested using the 69 years of 5-minute rainfall data recorded at Bochum, Germany. The mean, variance, covariance, skewness, and rainfall intermittency were well reproduced at the timescales from 5 minutes to a decade without any systematic bias. The extreme values were also well reproduced at timescales from 5 minutes to 3 days. The past-7-day rainfall before an extreme rainfall event, which is highly associated with the extreme flow discharge was reproduced well too. The rainstorm shuffling approaches introduced here may be adopted as a standard procedure in combination with any Poisson cluster rainfall model. The methods are simple and parsimonious, yet significantly reduce the systematic underestimation of rainfall variance at coarse scales, and improve the reproduction of skewness, and extreme rainfall depths values at a range of time-scales, thereby addressing well-known shortcomings of Poisson cluster rainfall models.

Keywords: Poisson cluster rainfall model; rainfall variability; timescale; holistic approach

1. Introduction

Most natural and anthropogenic systems react sensitively to a distinct range of rainfall temporal variability. Fine-scale rainfall temporal variability (e.g. several minutes to a day) influences flash floods (Singh, 1997; Oh et al., 2016; Anh et al., 2019) and subsequent transport of contaminants (Marshall et al., 2000) and sediments (Tucker et al., 2000). Coarse-scale rainfall variability (e.g. several days to years) influences water shortage (Gommes and Petrassi, 1996), human health (Patz et al, 2005; Kovats et al, 2003), food insecurity (Ayoub, 1999) and the corresponding human adaptation (Barbier et al, 2008) and migration (Afifi et al, 2015, Milan and Roano, 2014), as well as human adaptation strategies to recurring floods (Yu et al., 2014).

For this reason, most of the current system management strategies are established based on rainfall models designed to reproduce the rainfall variability at a limited range of time scales. However, the *real* natural and anthropogenic phenomena are the consequences of complex interactions of various components that are influenced by rainfall variability at a wide range of timescales. Therefore, a thorough understanding of the systems and comprehensive system management plans may only be achieved by employing a modelling framework that encompasses all relevant components based on one single rainfall model that captures the variability at all relevant timescales.

However, most rainfall models have an intrinsic limitation derived from their fundamental assumptions that do not precisely reflect the complex physical rainfall generation process, so they can reproduce the variability only within a limited range of timescales. For example, models based on the autoregressive process (Mishra and Desai, 2005; Modarres and Ouarda, 2014; Yoo et al., 2016) are good at reproducing the observed rainfall variability at timescales greater than 1 month, and the Markov chain models (Haan et al., 1976; Kwon et al., 2009), alternating renewal processes (Bernardara et al., 2007), and generalized linear models (Coe and Stern, 1982; Beecham et al., 2014; Chander and Wheater, 2002) cannot reproduce the observed variability at timescales finer than 1 day.

Poisson cluster rainfall models can reproduce the rainfall variability at timescales ranging from several minutes to several days (Marani et al., 2000; Park et al., 2019).

Several studies tried to overcome this issue by coupling multiple rainfall models. Koutsoyiannis (2001) suggested a novel coupling algorithm combining two seasonal autoregressive models with different temporal resolutions. He argued that the recursive application of the algorithm can produce a rainfall time series preserving the first- to the third-order moments of the observed rainfall at hourly to daily timescales. Menabde and Sivapalan (2000) combined the coarse-scale alternating renewal process model with a fine-scale multiplicative cascade model. Their model reproduced the scaling behaviour of extreme events up to a temporal resolution of 5 minutes. Fatichi et al. (2011) combined an autoregressive model with a Poisson cluster rainfall model (Rodriguez-Iturbe et al., 1987, 1988). Their composite model showed improved performance in reproducing the interannual rainfall variability that the latter often fails to capture. Kim et al. (2013a) disaggregated the monthly rainfall that is drawn from a Gamma distribution using the Poisson cluster rainfall model. They found that their composite approach helps reproduce not only the rainfall variability at hourly through yearly timescales, but also the statistical behaviour of rainfall annual maxima and extreme values at timescales ranging from 1 to 24 hours. Paschalis et al. (2014) combined a Markov chain model or Poisson cluster rainfall model for large timescales (e.g. daily) and a multiplicative random cascade model for fine timescales (e.g. minute), which outperformed the individual models across a wide range of scales. Park et al. (2019) suggested a method to combine the Seasonal Auto-Regressive Integrated Moving Average (SARIMA) model for monthly rainfall generation and the Poisson cluster rainfall model for hourly rainfall generation. Their model successfully reproduced the mean, variance, covariance, and proportion of dry periods of the observed rainfall at 1 hourly to yearly timescales at 15 locations across the United States.

Another research avenue addressing this topic stems from the recognition that the statistical distribution characterizing observations at a given timescale are distinct from one another. Papalexiou et al. (2018) suggested an algorithm of disaggregating a coarse time series into any finer temporal aggregation level while keeping the statistical properties of both fine and coarse timescales. Their algorithm replaces the observations at coarse timescales with a set of randomly placed blocks. Here, the blocks are randomly drawn from a normal distribution. They employed the unique parametric algorithm of Papalexiou (2018) for the transformation between the parent normal distribution and the distribution of the target variable. Their model successfully disaggregated the 30 years of monthly precipitation observed at a ground gauge in Kentucky, USA, to an hourly one while preserving moments of order one to three of the depth distribution, as well as the proportion of dry periods at all intermediate timescales.

The aim of this study is to show how one can preserve the main advantage of Poisson-cluster models (Rodriguez-Iturbe et al., 1987; 1988; Cowpertwait 1991; Onof and Wheater, 1993; Cowpertwait 1995; Kaczmarska et al., 2014; Onof and Wang, 2019), i.e. their storm-cell structure emulating the organisation of observed rainfall, while reproducing statistics over a similar range of scales. Poisson cluster rainfall models generate the rainfall time series with the assumption that the rainstorms arriving according to a Poisson process contain a series of rainfall cells with random depths and durations (Figure 1). This unique approach of conceptualizing rainfall based on the physical storm structure ensures that the model reproduces many statistical properties of the observed rainfall at timescales ranging from several minutes to several days (Olsson and Burlando, 2002). The performance of the model has been validated using rainfall data across the world, with a variety of climatological characteristics (Onof et al., 2000; Koutsoyiannis and Onof, 2001; Cowpertwait et al., 2007; Burton et al., 2008; Kim et al., 2013; Kim et al., 2016).

However, Poisson cluster rainfall models have an intrinsic limitation in reproducing the rainfall variability at time scales coarser than several days, which leads to the underestimation of extreme values at large time scales. Before further investigating this matter, note that the variance of a time series at a coarse time scale consists of the two distinct components coming from the independence and the correlation of the fine-scale records according to the following equations:

$$Var\left(Y_k{}^{(nh)}\right) = \sum_{i=(\mathrm{k}-1)\mathrm{n}+1}^{kn} Cov\left(Y_i^{(h)}, Y_i^{(h)}\right) + \sum_{i=(\mathrm{k}-1)\mathrm{n}+1}^{kn} \sum_{j=(\mathrm{k}-1)\mathrm{n}+1, j\neq i}^{kn} Cov\left(Y_i^{(h)}, Y_j^{(h)}\right)$$

$$= nVar\left(Y_1{}^{(h)}\right) + 2\sum_{i=(\mathrm{k}-1)\mathrm{n}+1}^{kn} \sum_{j=(\mathrm{k}-1)\mathrm{n}+1, j>i}^{kn} Cov\left(Y_i^{(h)}, Y_j^{(h)}\right) \qquad (1)$$

, where $Y_i^{(h)}$ represents i[th] value in a stationary rainfall time series at the aggregation interval h and n represents the degree of time series aggregation.

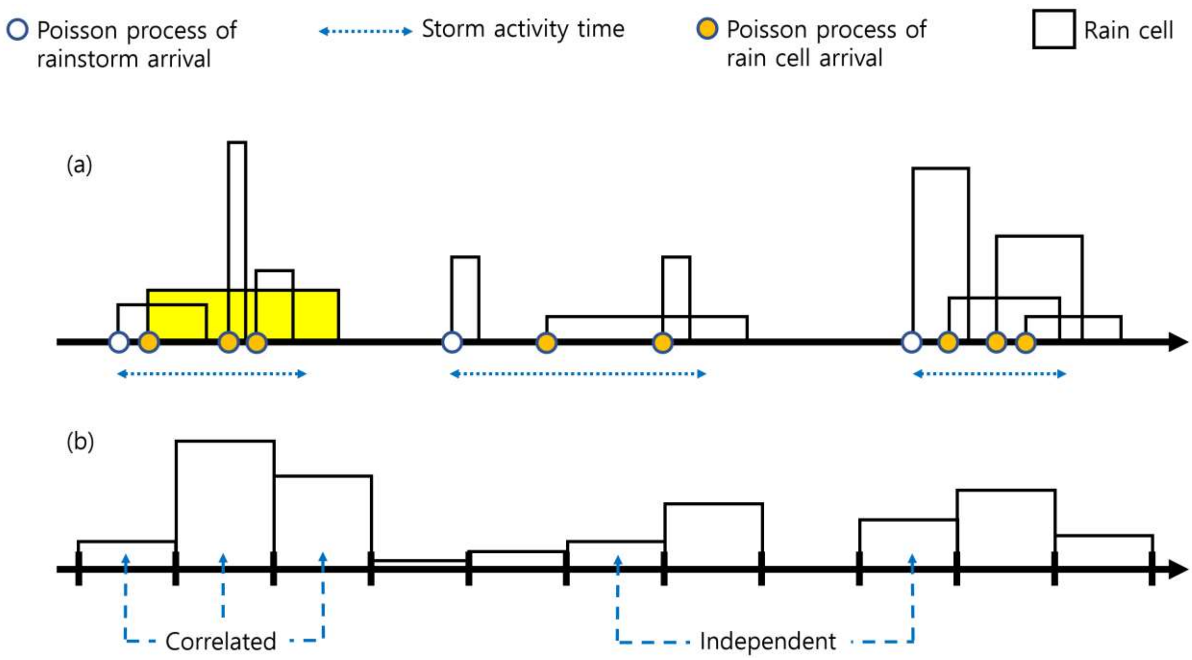

Figure 1. (a) Schematic of the Poisson cluster rainfall model. (b) aggregated time series over a given temporal interval. The aggregated values sharing the same rain cell (e.g. shaded in yellow) are correlated with each other while those not sharing the same rain cell are independent with each other.

Note that the second term of the right-hand side of the equation represents the correlation between *all* fine-scale records for time lags smaller than or equal to the relevant coarse scale. If this correlation is underestimated by a model, the variance of the coarse-scale time series, the left-hand side of Equation 1, will be also underestimated. To see why this might be the case, consider Figure 1b, which shows the aggregated time series of the storm and the cell structure modelled by the Poisson cluster rainfall models (Figure 1a). The figure shows that the values in the aggregated time series will be correlated with each other if they share the same rain cell (shaded in yellow colour in Figure 1a). On the contrary, they will be independent if the values do not share the same rain cell. This happens in particular when these cells belong to different non-overlapping storms (the probability of storms overlapping is tiny). This means that Poisson cluster rainfall models have the inherent limitation of not being able to reproduce the fine-scale correlation[1] between rainfall values observed at distant times that is observed, for instance with monsoon rainfall (Singh et al., 1981), soil moisture recycling (Eltahir, 1998; Entekhabi et al., 1996; Kim and Wang, 2007) and as a result of large-scale global atmospheric circulation (Mooley and Parthasarathey, 1984; Carvalho et al., 2004; Berkelhammer et al., 2010). Equation (1) shows that this leads to the underestimation of the variance at coarse timescales.

This investigation also leads to the conjecture that, if Poisson cluster rainfall models are adjusted so that they can account for the correlations between rainfall values observed at distant times, the issue of underestimating large timescale rainfall variability will be resolved. The rainfall model being proposed here was developed based on this principle. The model is composed of three sub-modules each of which is designed to reproduce the rainfall correlation over a range of timescales (i.e. 5 minutes to a couple of days, a couple of days to one month, and one month to a decade) reflecting the realistic storm features associated with internal storm structure, summer monsoon, soil moisture recycling, and the large scale global atmospheric circulations. The separation of these ranges of timescales is loosely connected to observed breaks in the scaling behaviour of rainfall detected by multiscaling analyses of rainfall depths (e.g. de Lima and Grasman, 1999; Marani, 2005). The proposed model was tested with 69 years of 5-minute rainfall records observed in Bochum, Germany.

2. Methodology

2.1. Data Description

[1] This is also true of coarse-scale correlations; here we initially focus upon fine-scale correlations. Below, we will see how one can also increase correlation at coarser scales.

This study used the 69 years of 5-minute rainfall data observed at Bochum, Germany for the period between January 1st, 1931 and December 31st, 1999. The mean monthly rainfall displays a clear seasonality and varies from 54cm in March to 82cm in July. The data have approximately 1 percent of missing periods that are distributed over the years and the calendar months (Figure 2a). The months with the missing periods greater than 0.1 percent were excluded from the analysis.

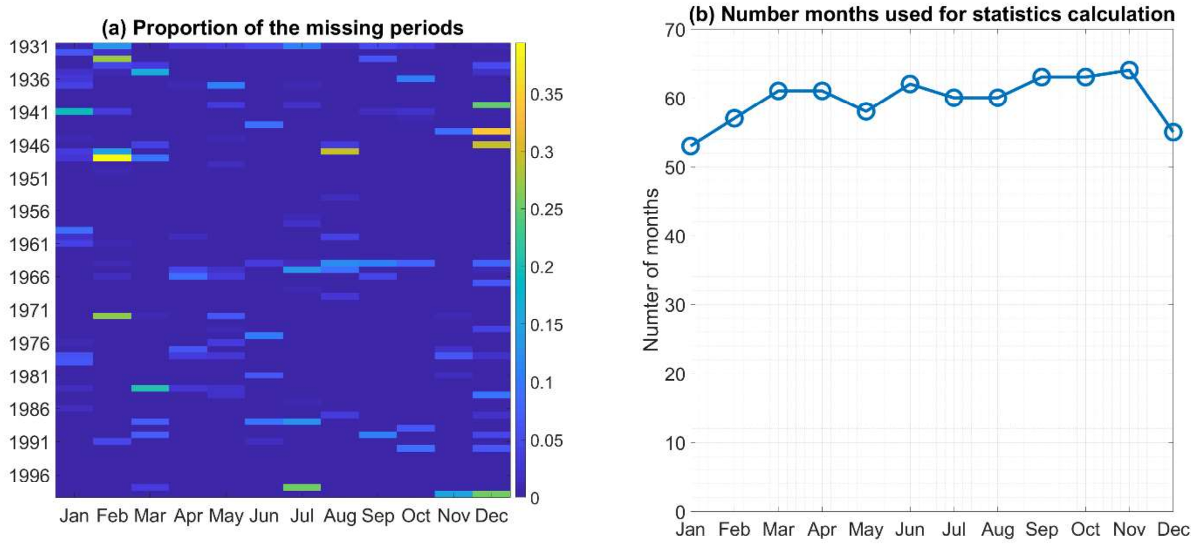

Figure 2. Proportion of the missing periods varying with calendar months and year of the 5-minute Bochum rainfall data.

2.2. Model Description

The first module generates the fine-scale rainfall time series using a randomised Bartlett-Lewis rectangular pulse version of the Poisson cluster rainfall model. Then, the second module shuffles the sequence of the rainstorms to reflect the rainfall variability at time scales ranging from a couple of days to one month. The third module rearranges the adjusted sub-monthly rainfall so that it can reflect the observed rainfall statistics at time scales coarser than one month.

2.2.1. Module 1: Fine scale rainfall generation

For the generation of fine-scale (e.g. sub-hourly) rainfall, this study uses a recent version of the Randomised Bartlett-Lewis Rectangular Pulse (RBLRP) model of Kaczmarska et al. (2014) since it has been shown to outperform other types of Bartlett-Lewis models (ibid.; Onof and Wang, 2019).

Unlike the non-randomised BLRP model (Rodriguez-Iturbe et al., 1987) and the traditional randomised RBLRP model (Rodriguez-Iturbe et al., 1988), the $RBLRP_x$ model introduces an the inverse correlation between rainfall cell duration and intensity, in line with the observed behaviour of intense convective rainfall lasting several minutes and milder frontal rainfall lasting for several days. The model generates rainfall based upon the following sequences:

(1) A series of rainstorms arrives in time according to a Poisson process. The parameter of the Poisson process is λ [1/T].

(2) The temporal scaling factor η [1/T] is a gamma distributed random variable with shape and rate parameters ν [-] and α [1/T] respectively. This scaling factor is used as parameter of the exponential distribution of cell durations and to determine the distributions of rainstorm activity duration, rain cell depth, and rainfall cell arrival. All these random variables are mutually independent, which implies in particular that total storm rainfalls are mutually independent.

(3) For each rainstorm and conditionally upon η, the storm activity time is an exponentially distributed random variable with parameter $\eta\phi$, where ϕ [-] is a model parameter.

(4) For each rainstorm and conditionally upon η, rain cells arrive according to a truncated Poisson process with the parameter $\eta\kappa$ where κ [-] is a model parameter. The truncation is defined by the storm activity duration: rain cells can arrive only before the termination of the storm activity duration.

(5) Each rain cell is assigned a duration which is an exponentially distributed random variable with parameter η [1/T].

(6) Each rain cell is assigned an intensity that is a random variable whose distribution could e.g. be exponential, gamma or Pareto. Its mean is $\iota\eta$ where ι [L] is a model parameter. In the present study, we choose the Gamma distribution with shape parameter ω [-] and scale parameter $\iota\eta/\omega$.

The model is thus characterised by the following seven parameters: λ [1/T], ν [-], α [1/T], ι [L], ϕ [-],κ [-], and ω [-].

The parameters of the $RBLRP_x$ model (the "RBL" model hereafter for simplicity) are calibrated such that the statistics of the synthetically generated rainfall approximate those of the observed rainfall. Kaczmarska et al. (2014) derived the analytical expression of the first- to the third-order central moments of the synthetically generated rainfall, and Onof and Wang (2019) further developed the equations to extend the search domain of the parameter α (α<1), which improved reproduction of both extreme and standard statistics at fine timescales (e.g. hourly and sub-hourly). The analytical expression of the proportion of dry (or wet) periods derived by Rodriguez-Iturbe et al. (1988) was also included the calibration.

A variant of the particle swarm optimization algorithm (Cho et al., 2011) was used to identify the parameters which minimise the following objective function:

$$\mathrm{OF} = \sum_{i=1}^{n} w_i\left[\widehat{M_i} - M_i\right]^2 \qquad (1)$$

,where $\widehat{M}_i$ and M_i for $i = 1, \dots, n$ respectively represent the n modelled and observed rainfall statistics selected for use in the calibration, and w_i for $i = 1, \dots, n$ represent the weight factors given to each statistic.

The M_is used for the calibration in this study are the mean, variance, covariance, skewness, and proportion of wet periods at 5-, 10-, 15-, 30-, 60-, 120-, 240-, 480-, 960-, 1440-minute aggregation, so n is 50 (5 different statistics x 10 aggregation intervals). The calibration was performed separately for each calendar month. The weight factors w_i may be determined in various manners depending on the purpose for which the synthetic rainfall is to be used (Kim et al., 2012). In this study, each weight factor w_i is determined as the inverse of the variances of the corresponding observed property M_i: i.e.. using the following equation:

$$w_i = \frac{m}{\sum_{y=1}^{m}\left[M_i^y - \overline{M_i}\right]^2} \quad (2)$$

, where M_i^y represents the i[th] statistic of a given calendar month of year y; $\overline{M_i}$ represents the mean of M_i^y over the years; and *m* represents the number of years of observation.

This entails that statistics with greater inter-annual variability have less weight. This choice has been shown to define an optimal generalized method of moments (Jesus and Chandler, 2011)

Table 1. Parameters of the RBL model for the calibration period (1930-1964).

Month	λ	ν	α	ι	ϕ	κ	ω	OF(Eq.1)
1	0.001294	0.004906	1.0650	0.0259	0.000142	0.02771	2.9804	3.9014
2	0.001129	0.005375	1.1289	0.0278	0.000109	0.02125	0.6163	2.2788
3	0.001482	0.013439	1.0958	0.0449	0.000425	0.03662	0.7988	3.0768
4	0.000960	0.003882	1.0510	0.0485	0.000081	0.01000	0.5993	3.8287
5	0.001343	0.005118	1.0390	0.0395	0.000324	0.03772	0.1980	3.8751
6	0.001819	0.065766	1.2424	0.0101	0.004000	1.84105	0.0100	5.9534
7	0.001693	0.031617	1.1690	0.0100	0.002943	1.39931	0.0129	5.9653
8	0.000717	1.000000	1.1447	1.0001	0.004000	0.03517	0.4096	3.2342
9	0.000585	0.452496	1.0485	1.0005	0.001000	0.01000	1.0179	6.9052
10	0.001153	0.009338	1.1275	0.0547	0.000221	0.02268	0.7556	3.0301
11	0.000814	0.001761	1.0459	0.0254	0.000029	0.01000	1.5975	9.1794
12	0.001359	0.010000	1.0788	0.0397	0.000241	0.03020	0.5082	4.4151

2.2.2. Module 2: Rainstorm shuffling

This module shuffles the rainstorms generated by the RBL model. Figure 3 describes the shuffling process. The rainstorms are shuffled based on the following sequence:

(1) While generating the fine-scale rainfall in the Module 1, the time of the rainstorm occurrence and the set of rain cells contained in each of the rainstorms are stored in the database.

(2) Empty the original time series except for the occurrence times of the rainstorms.

(3) Randomly select a rainstorm from the database and place it at the location of the first rainstorm occurrence. Here, each of the rainstorms has the same probability of being selected. The selected storm is then excluded from the database.

(4) Another storm is chosen from the database and placed at the next storm occurrence location. Here, the probability P_i of the rainstorm i being selected, is given by the following equation:

$$P_i = \frac{1}{\sum_{k=1}^{n_i} S_k} \cdot S_i \tag{4}$$

$$\text{where } S_i = \left[\frac{1}{|\log(Q_i/Q_{prev})|}\right]^{\delta} \tag{5}$$

and Q_i and Q_{prev} represent the total depths of the i$^{\text{th}}$ rainstorm and that of the previously selected rainstorm respectively. Q_i is calculated as follows:

$$Q_i = \sum_{j=1}^{n_c} \left(I_{i,j} \cdot D_{i,j}\right) \tag{6}$$

, where $I_{i,j}$ and $D_{i,j}$ represent the intensity and the duration of the rain cell, respectively, and the first and the second subscripts are the indices corresponding to the rainstorm and the rain cell respectively. For example, $D_{i,j}$ represents the duration of the j^{th} rain cell contained in the i^{th} rainstorm. n_c represents the total number of rain cells contained in the rainstorm. S_i represents the similarity between the i^{th} rainstorm and the previously selected rainstorm. n_i is the number of rainstorms remaining in the database at stage i of the process. δ is a model parameter to be calibrated. The selected storm is then excluded from the database.

(5) Step (4) is repeated until the entire storm occurrence places in the time series are filled with selected rainstorms.

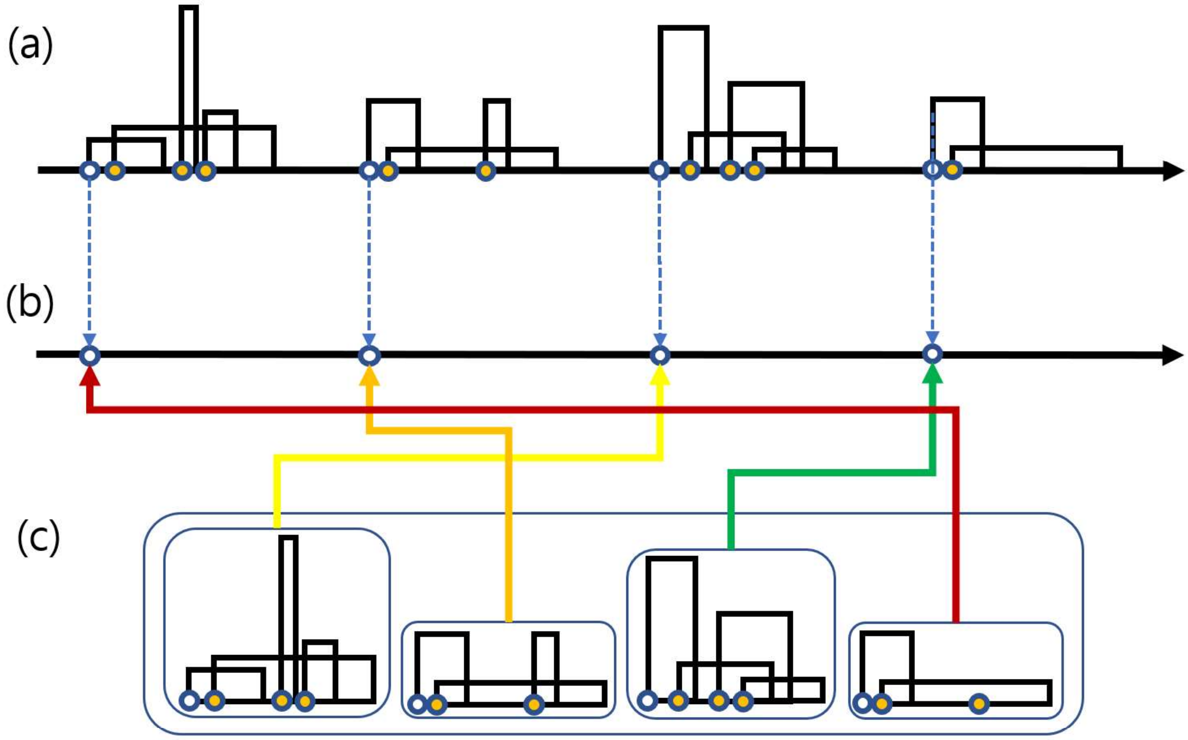

Figure 3. The schematic of the storm shuffling algorithm of Module 2. (a) The original fine scale rainfall time series. (b) The rainstorms are removed from the original time series, but the times of the rainstorm occurrence in the time series are kept. (c) The rainstorms are randomly selected and placed back into the timeseries. Here, rainstorms with a depth resembling that of the previously selected rainstorm have greater probability of being selected, according to the probability defined in step (4).

Probability P_i (Equation 5) is designed to reflect the similarity in the depths of successive rainstorms characterising the observed rainfall. After this shuffling, it is therefore more likely that storms with relatively similar total depths follow one another. This algorithm amounts to altering the RBL model by replacing the assumption of storm independence, with that of a dependence between consecutive total storm rainfalls defined by the conditional probabilities P_i. The other assumptions of the RBL model remain valid.

The rainstorms occur at times defined by the storm arrival Poisson process of the RBL model, and each of the selected rainstorms selected for relocation at each rainstorm occurrence time has of course already been generated in the simulation of the RBL model (see Section 2.2.1). Hence, the statistical properties of the wet-dry process as well as of the marginal depth distribution (mean, variance, skewness) at scales finer than the typical storm duration are largely unaffected by this reshuffling. For larger scales, all but the mean depth will be altered. However, the alteration is small as shown in Figure… The autocorrelation structure is also affected by the shuffling process, at least for scales and time-lags whose product exceeds the typical storm duration, but again the effect is small as seen in Figure …

Note that the probability P_i could be adjusted so as to reflect the similarity of not only depth but also duration of storms. This would, for instance, enable this reshuffling process to enable the generated rainfall to reflect the rainfall characteristics of the monsoon season, during which long-duration rainfall events successively occur.

Model parameter δ represents the impact of the degree of similarity between the successive rainstorms, as characterised by the modulus of the logarithm of the ratio of their total depths $\left|\log\left(Q_i/Q_{prev}\right)\right|$. It is calibrated separately from the RBL parameters so that the monthly variance of the shuffled synthetic rainfall time series resembles that of the observed rainfall. An analytical approach to the calibration could not be implemented due to the absence of the equation representing the monthly variance of the shuffled synthetic rainfall. Therefore, the pattern search optimization algorithm (Audet and Dennis, 2002) was used to minimize the objective function that is numerically calculated in the following manner:

(1) 300 months of 5-minute rainfall time series are generated using Module 1.
(2) The original synthetic rainfall time series is shuffled based on a given value of δ.
(3) The shuffled 5-minute rainfall time series is aggregated to monthly rainfall, and the variance of the aggregated monthly rainfall is calculated.
(4) The objective function value is calculated as the absolute value of the difference between the observed monthly rainfall variance and the synthetic monthly rainfall variance.

Figure 4a shows the relationship between δ and the variance of the shuffled synthetic rainfall aggregated to the monthly level. The parameter of July of the study area was used to generate the fine-scale rainfall. The figure a general increase of the variance as a function of δ. This is because, as δ increases, a greater value of P_i is assigned to the rainstorms with the depth similar to the previous rainstorm, so the greater δ value, the more similar rainstorms flock together, which increases the occurrence of both wet and dry months, thereby increasing the monthly variance.

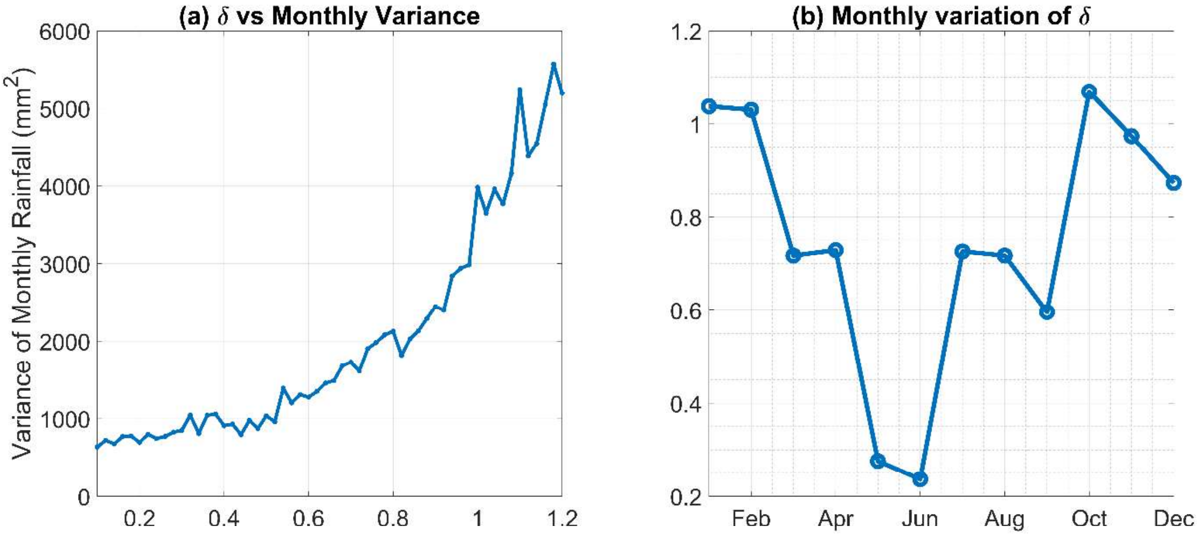

Figure 4. Relationship between δ and the variance of the monthly rainfall depth.

Note that the two variables do not have a smooth relationship because the variance shown in the y-value is calculated from the stochastically generated rainfall. For this reason, the pattern-search optimisation algorithm was employed, to identify the optimal parameters in the objective function surface with random sampling noise. Figure 4b shows the calibrated δ for each of the calendar months. This exhibits a clear seasonal trend. Since greater δ values represent greater inter-storm correlations, this result reveals that consecutive summer rainfall events of the study area are less likely to resemble one another in terms of total storm depth, and vice versa for the winter rainfall events, which is to be expected.

2.2.3. Module 3: Monthly rainfall shuffling

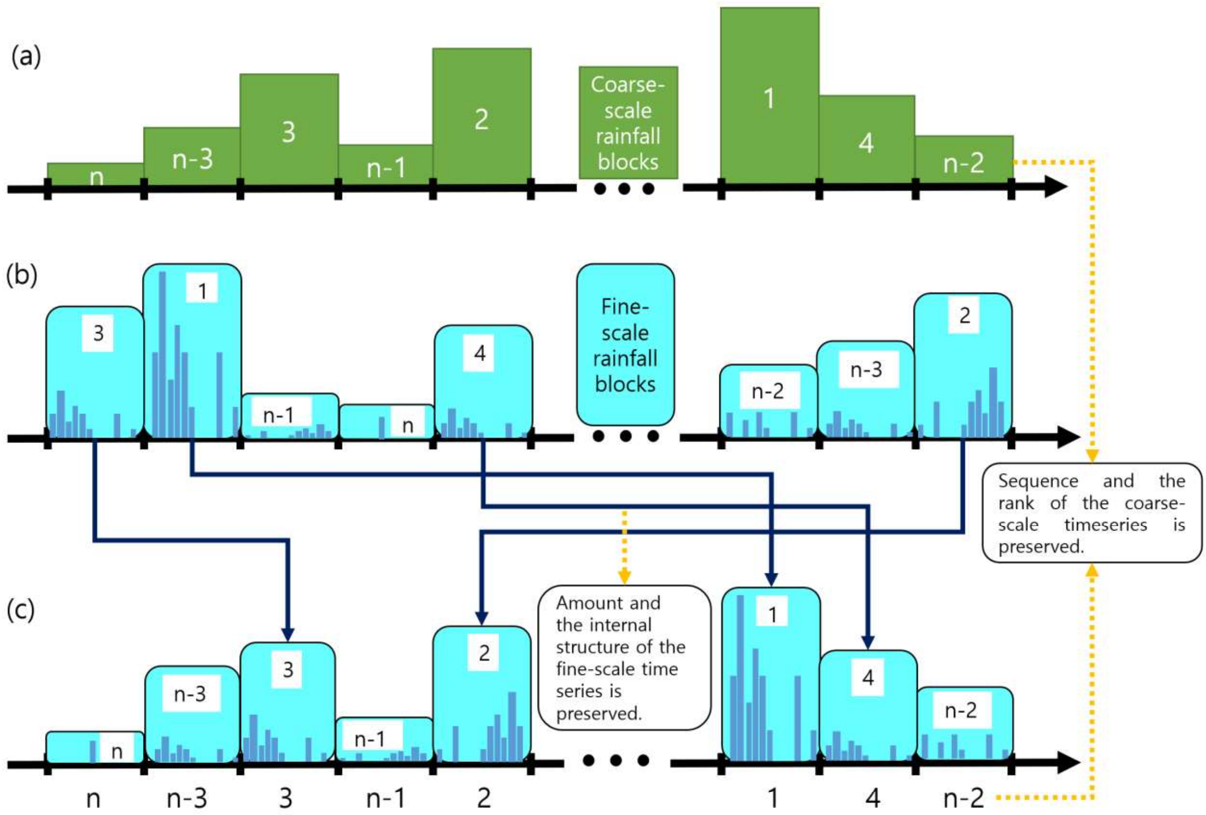

Figure 5. The schematic of Module 3 of the model. (a) A monthly rainfall time series is generated using a coarse-scale model (e.g.the SARIMA model). (b) The Fine scale time series is segmented into monthly blocks. (c) The final time series is composed by adopting the sequence and rank of the coarse-scale time series and the amount and the internal structure of the fine-scale time series.

Figure 5 describes the process involved in Module 3. This module rearranges the stochastically generated rainfall time series so that it can account for the variability at timescales greater than 1 month following the steps described below:

(1) The monthly rainfall time series is generated for the same length as the fine-scale rainfall time series using a separate coarse-scale rainfall model. Any coarse scale model can be used. Here, we call each of the monthly rainfalls generated by the coarse-scale model, a “coarse-scale rainfall block” (Figure 5a).

(2) The shuffled synthetic fine-scale rainfall time series is segmented into different calendar months and years. Here, we call each segment as “fine-scale rainfall block” (Figure 5b).

(3) The quantile matching between the fine-scale rainfall blocks and the coarse-scale rainfall blocks is performed based on the total rainfall depth for each of the months of a given calendar month. For example, the fine-scale rainfall block with the n^{th} greatest depth is placed in the location of the coarse-scale rainfall block with the n^{th} greatest depth of the same calendar month. This process is repeated for all 12 calendar months (Figure 5c).

This study uses the Seasonal Auto-Regressive Integrated Moving Average (SARIMA) model for monthly rainfall generation. The model structure is as follow:

$$\mathrm{ARIMA}_{(p,d,q)(P,D,Q)} = \mathrm{ARIMA}_{(0,0,0)(3,0,3)}$$

,where p and P represent the degrees of the nonseasonal and seasonal autogressive polynomials respectively; q and Q represent the non-seasonal and seasonal moving average polynomials respectively; and d and D represent the non-seasonal and seasonal degrees of differencing in the linear time series. Note that the optimal model structure of (p,d,q)(P,D,Q) = (0,0,0)(3,0,3) is only valid for the monthly rainfall data investigated in this study. They were determined through an optimization process to minimize the Akaika Information Criterion (AIC) in the parameter space where p, d, q, P, D, and Q discretely vary between 0-2, 0-2, 0-2, 0-9, 0-1, and 0-9, respectively.

The shuffling algorithm suggested here adopts the sequence and the ranks from the blocks of the coarse-scale time series while it borrows the amount and the temporal structure from the fine scale rainfall time series internal to the blocks. Here, the key to a seamless coupling between the two models is whether the marginal distribution of the amounts of fine scale rainfall aggregated to the monthly level match the distribution of the amounts of monthly rainfall generated by the coarse scale model, at least up to the second-order. While the means of both distributions are identical because they are reproduced by the RBL model at all time-scales, Module 2 ensures a match at the second-order because the parameter δ of Module 2 is calibrated so as to preserve the variance of observed monthly rainfall, which the SARIMA model of Module 3 is also designed to reproduce.

For convenience, we define the names of the models depending on the level of processing as follows:

(1) RBL: The Randomized Bartlett-Lewis model (Module 1 only)

(2) RBL-S: The RBL model with Module 2 (rainstorm shuffling algorithm)

(3) RBL-S2: The RBL model with Module 2 and Module 3 (both rainstorm shuffling and monthly rainfall shuffling algorithm)

2.3. Model application and validation

500 years of synthetic rainfall data were generated. Both the standard statistics and the extreme values were compared at timescales from 5-minutes to a decade.

3. Results and discussions

3.1. Reproduction of standard statistics.

Figure 5 compares the statistics of the observed (x) and the synthetic (y) rainfall at timescales ranging from 5 minutes to 6 years. The coloured triangles and grey discs represent the result of the RBL-S2 and the RBL models, respectively. The colours of the triangles and the brightness of the grey discs represent different aggregation intervals. Each colour has 12 triangles or discs representing each calendar month. For this, the time series of a given calendar month for consecutive years were constituted (e.g. January 1930, January 1931,…, January 1963 for the calibration period), then the time series were aggregated to a given timescale, from which statistics were calculated. For this reason, the timescales of 1, 3, and 6 months shown in this plot are 1, 3, and 6 years, respectively, which is denoted in the colour legend.

The mean rainfall is well reproduced regardless of the model type (and if this is true at one scale, it is true at all scales). The variance is well reproduced by both models at sub-hourly scales. The RBL model underestimates the variance for aggregation intervals exceeding approximately one hour and the degree of underestimation increases with the increase of the aggregation interval. The RBL-S2 model does not underestimate variances for any scales from 5 minutes to 6 years. This result suggests that the model also successfully reproduces the rainfall correlation structure across the timescales.

While the RBL model underestimates the skewness at time scales exceeding ~1hour, the RBL-S2 model significantly reduces the degree of underestimation. This is because the rainstorm shuffling algorithm of the RBL-S2 model makes the similar rainstorms flock together in the time series, which produces more of both smaller and greater rainfall depth values when the time series is aggregated to the coarser level. This not only increases the variance but also thickens both the head and tail part of the rainfall depth distribution increasing the skewness.

3.2. Correlation structure

Figure 6 compares the correlation structure of the time series of February rainfall. The red, blue, and black lines are the Auto-Correlation Function (ACF) corresponding to the observed rainfall, the synthetic rainfall generated by the RBL model, and the synthetic rainfall generated by the RBL-S2 model, respectively. The ACFs of the time series aggregated into 5 minutes, 30 minutes, 1 hour, 4 hours, 1 day, and 3 days are shown. The autocorrelation function (ACF) of the observed rainfall does not converge to 0 even at lag values corresponding to approximately 2 weeks (Figure 6e and 6f). This gradual decaying trend of the ACF could not be reproduced by the RBL model, of which the ACF converges to 0 at the lag values corresponding to approximately 2 days. This value roughly coincides with the inter-storm arrival time (λ^{-1}) which varies between 1.3 days (November) and 2.8 days (February). This is because, as the lag of the ACF increases, the rainfall values from independent rainstorms are considered in the calculation of the autocorrelation coefficient (See Figure 1b), which abruptly decreases the ACF value. Conversely, the RBL-S2 model successfully reproduces the gradual decaying tendency of the observed ACF. This is because the correlation between the rainfall values sampled from consecutive rainstorms tends to persist even though the lag of the ACF becomes longer than the inter-storm arrival time.

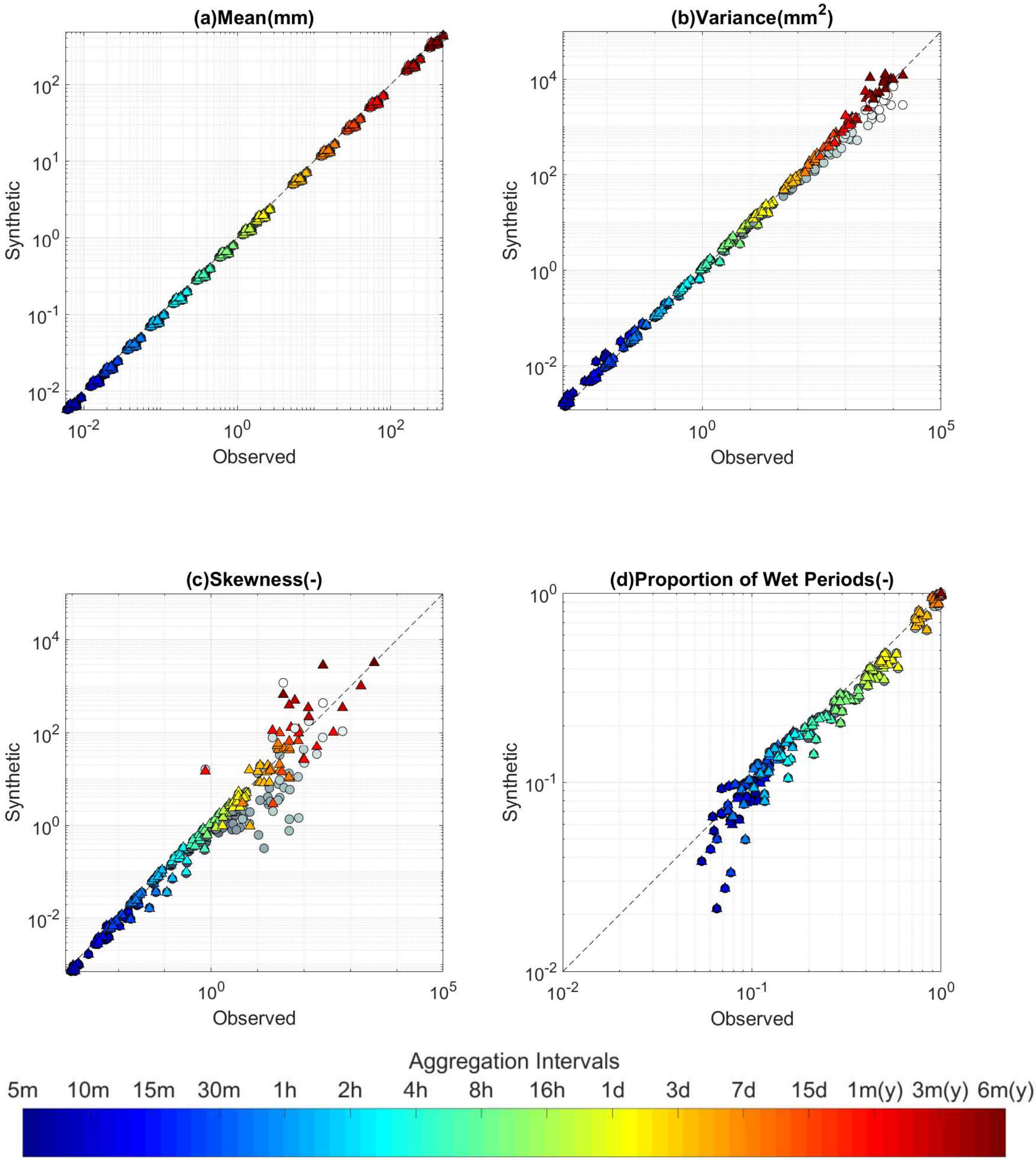

Figure 5. Mean, variance, skewness, and proportion of wet periods of the observed(x) and synthetic (y) rainfall time series. The coloured triangles and grey circles represent the RBL-S2 and the RBL models respectively. The colours of the triangles and the brightness of the grey circles represent different aggregation intervals.

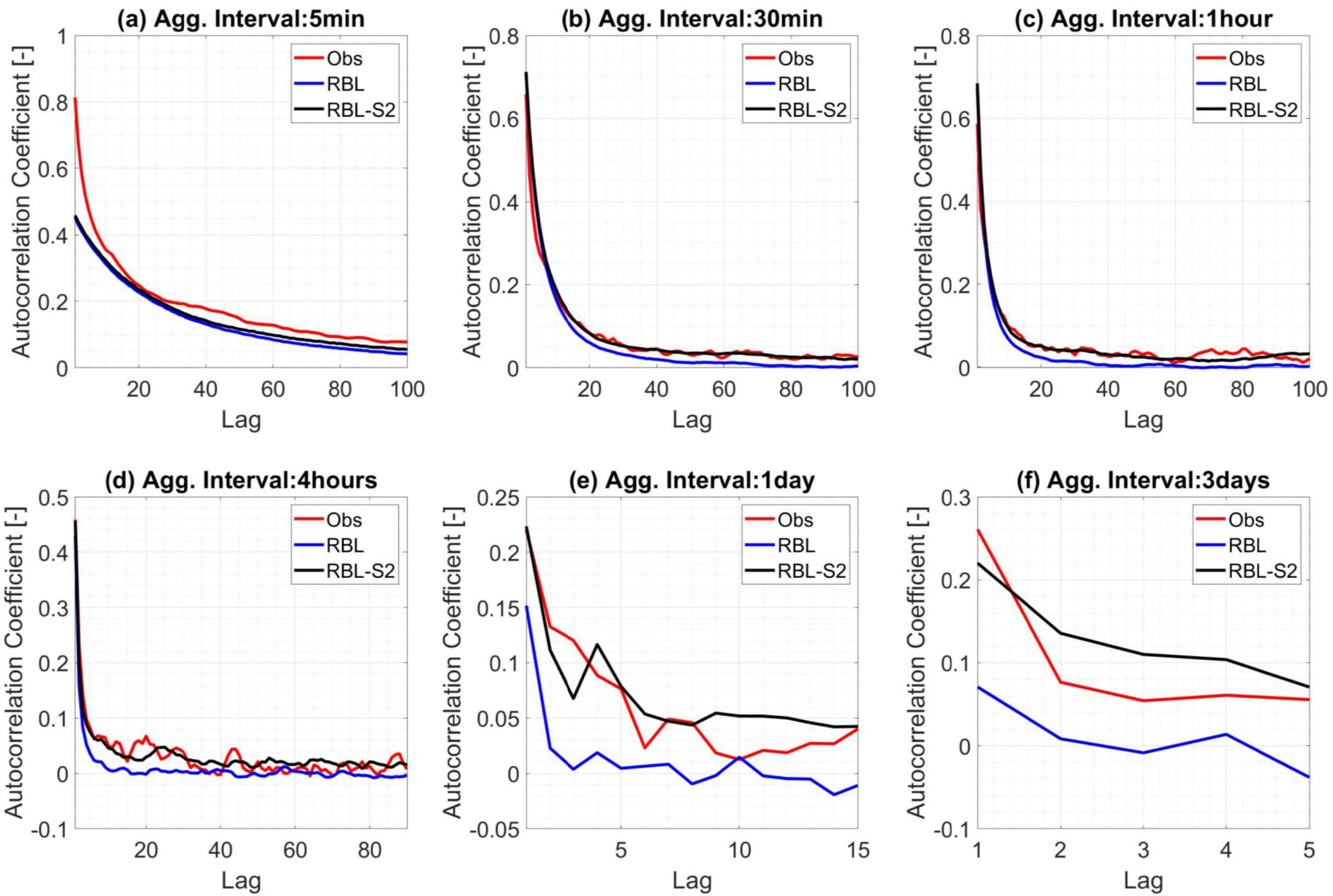

Figure 6. Autocorrelation function (ACF) of the observed and the synthetic rainfall time series of February. ACF plots with the aggregation interval of 5min, 30min, 1hour, 4hours, 1day, and 3days are shown.

3.3. Interannual variability

Figure 7 compares the quantiles of observed (x) and synthetic (y) monthly rainfall of January, April, July, and October. For all months, the RBL model overestimates the low monthly rainfall values (dry period wetter than the observation) and underestimates the high monthly rainfall values (wet period drier than the observation). The RBL-S2 model resolves this problem. This is also because the rainstorm shuffling algorithm makes large rainstorms flock together with large rainstorms and small rainstorms with small rainstorms, so the months with extremely large and low rainfall occur in sequence more frequently than the case of the RBL model where a series of rainstorms have independent characteristics.

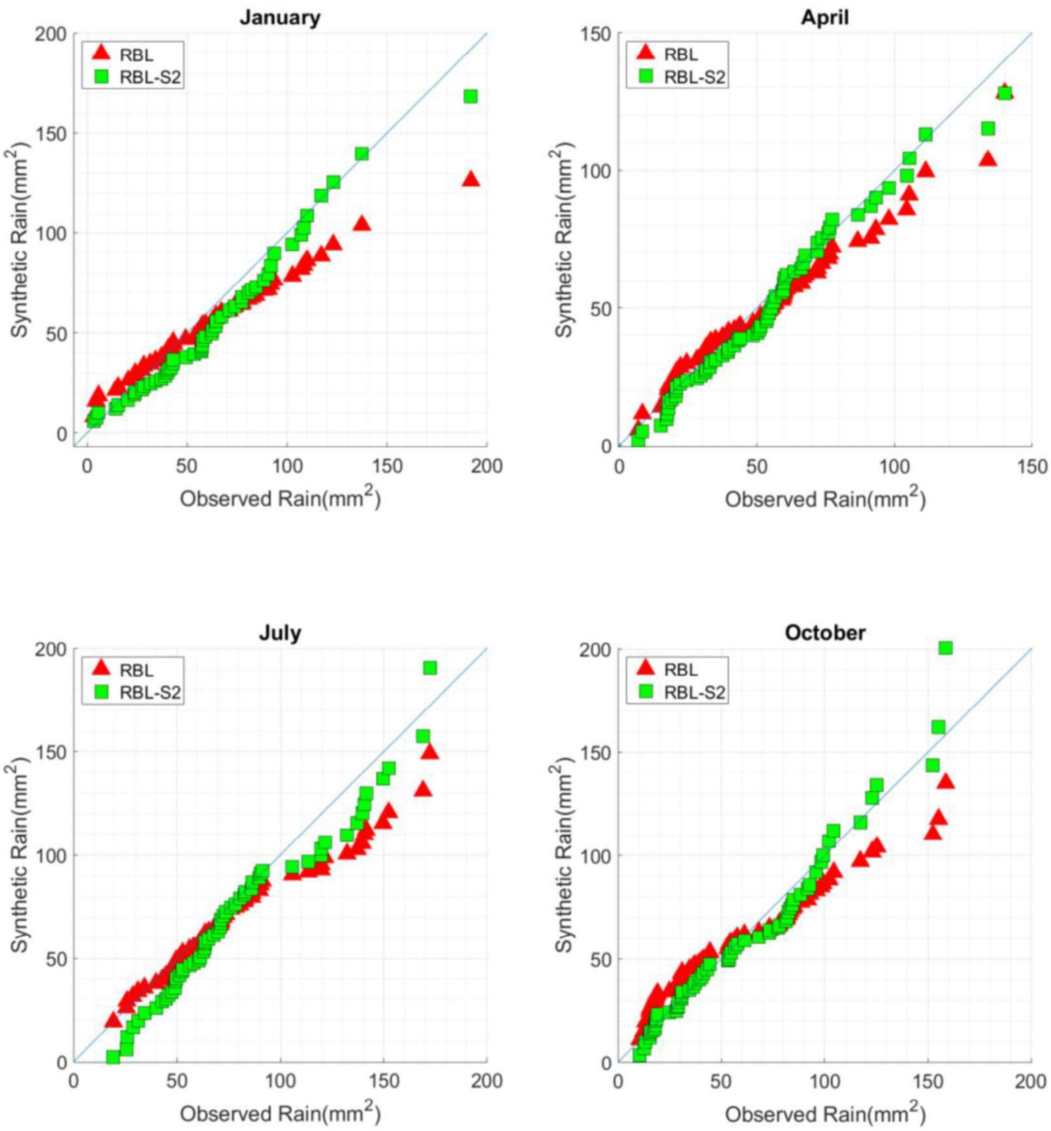

Figure 7. Comparison of the observed rainfall quantiles (x) and the synthetic rainfall quantiles (y) for January, April, July, and October monthly rainfall.

3.4. Variance across the timescales

The primary purpose of this study is to develop a rainfall model that can reproduce the rainfall variability at all hydrologically relevant timescales so it can simultaneously be applied to all components of the modelling system. Figure 8 compares the variances of the observed and the synthetic rainfall at aggregation intervals ranging between 5 minutes to a decade. While the RBL model underestimates the variance at timescales greater than approximately 1 day, the RBL-S model successfully reproduces the variances at time scales from 5 minutes to 6 months, but it also underestimates the variance at the timescale exceeding 6 months. The RBL-S2 model successfully reproduces the rainfall variability at timescales from 5 minutes to a decade. This is because the model reflects the rainfall variability at the large timescale (e.g. 1 to 10 years) that the SARIMA model of Module 3 reproduces.

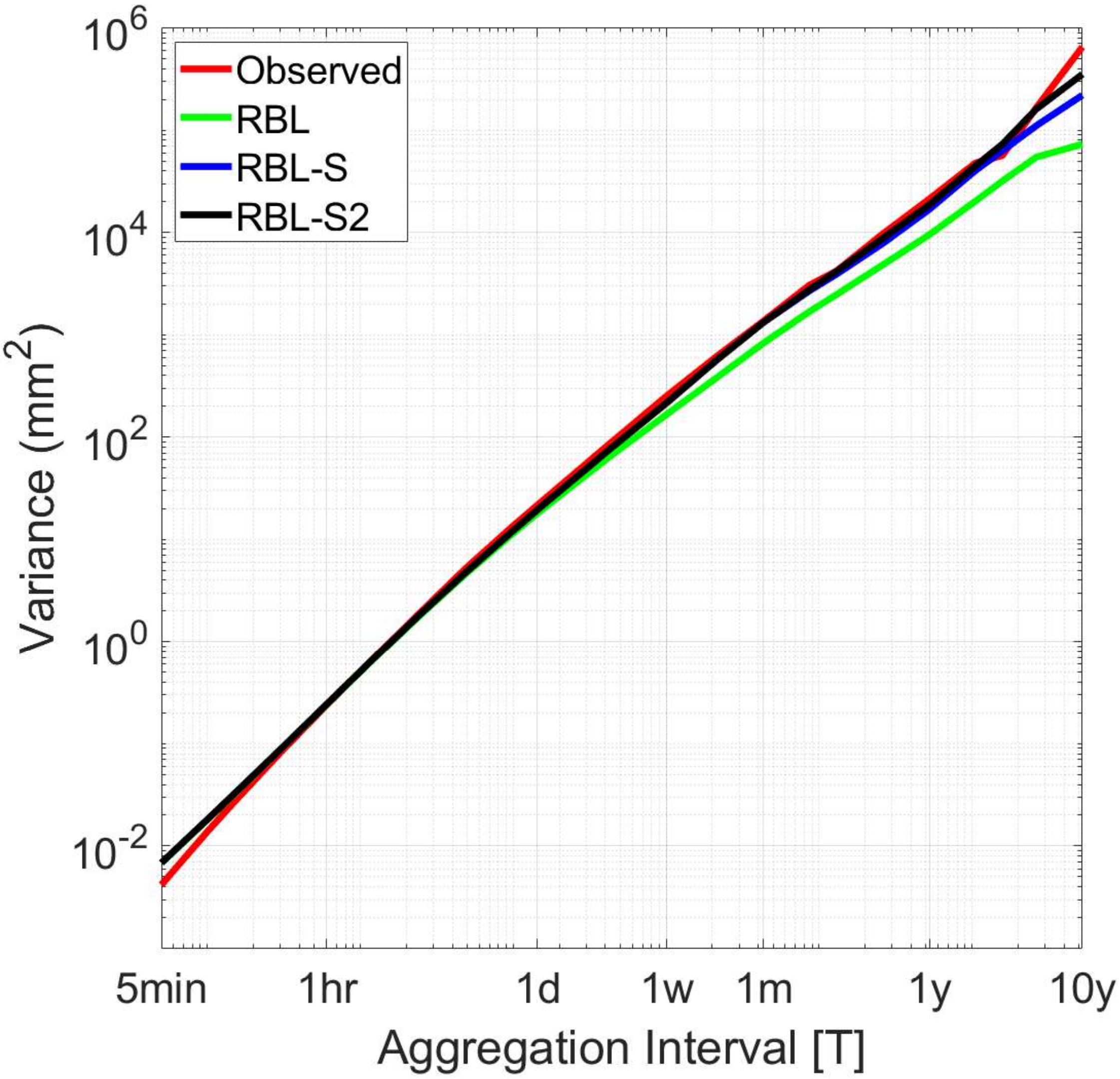

Figure 8. Variances of observed and the synthetic rainfall across the timescales ranging from 5 minutes to 2 years. The results based on the RBL, RBL-S, and RBL-S2 models are shown.

3.5. Extreme Values

Figure 9 shows the relationship between annual maximum rainfall depths and recurrence intervals for both observed and synthetic rainfall. The x-axis was scaled based on the Gumbel transformation yielding the reduced variate. The blue dots represent the observed rainfall and the red and the green solid line represents the synthetic rainfall generated by the RBL and the RBL-S2 model. Both models successfully reproduce the observed extreme values without a significant trend of over- or underestimation at sub-hourly timescales. This is a significant improvement compared to the previous studies which found that the Poisson cluster rainfall models tend to systematically underestimate the extreme values. They attributed the causes to the parsimonious nature of the model (Kim et al., 2013, Park et al., 2019), the model calibration scheme in which skewness of the rainfall depth distribution is not considered (Cowpertwait, 1998; Kaczmarscka et al., 2014; Onof and Wang, 2019), and the intrinsic limitation of the exponential distribution from which rain cell intensity values are drawn (Onof and Wang, 2019). The latter study found that the calibration scheme significantly affects the reproduction of extreme values, and suggested considering cell depth distributions other than the exponential.

As opposed to the RBL model of this study that considered the skewness in the calibration process and the Gamma rain cell distribution, the model based on the exponential rain cell distribution with no consideration of skewness (blue dashed lines in Figure 9) underestimated the 30-year rainfall by 38 percent and 41 percent at the 5 minute and 1 hour timescale, respectively. The one that considered the skewness but based on the exponential rain cell intensity (black dashed lines in Figure 9) underestimated the same values by 18 percent and 25 percent, respectively.

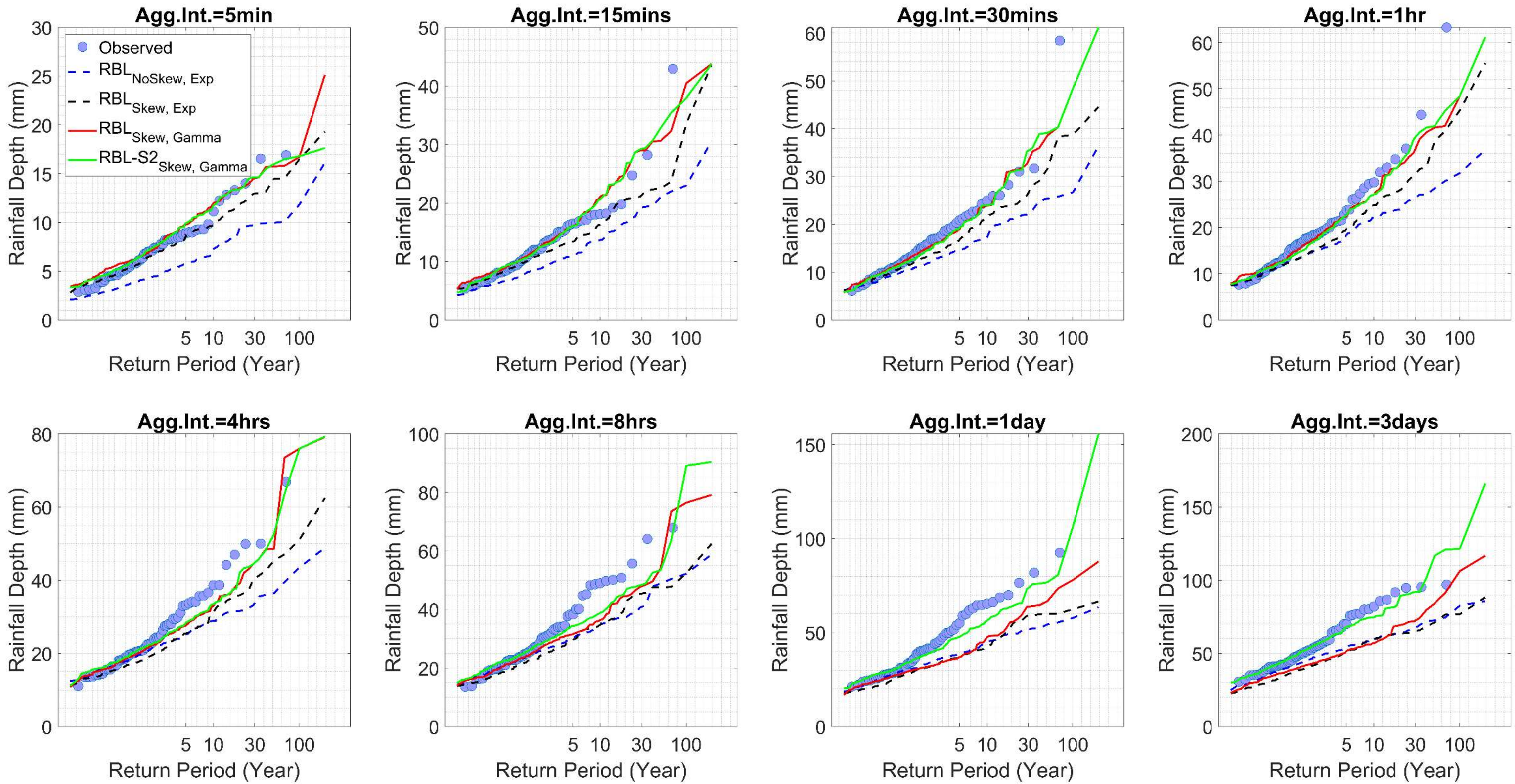

Figure 9. The relationship between the annual maximum rainfall depth and the recurrence interval at the timescales between 5 minutes and 3 days. The blue dots represent the observed data for the whole observation period (1930-1999), The red and green solid lines represent the synthetic rainfall generated by the RBL model and the RBL-S2 model of this study. The black dashed line represents the synthetic rainfall generated by the RBL model based on the exponential rain cell intensity and with skewness included in the parameter calibration. The blue dashed line represents the synthetic rainfall based on the exponential rain cell intensity and no consideration of skewness in the parameter calibration.

The extreme values at timescale between 4 hours and 1 day were underestimated by all models at the range of the recurrence interval between 5 years and 30 years. This trend of underestimation was reduced at the recurrence intervals exceeding 30 years. This is associated with the fundamental model structure of Poisson cluster models (See Figure 1a). Indeed, first, note that the average duration of the rainstorms according to the model structure ranges between 1.9 hours and 4.5 hours according to the equations derived by Onof (2003) and the parameter values in Table 1:

For a rainstorm to reproduce extreme rainfall at timescales that are much finer than the rainstorm duration (e.g. 5 minutes through 1 hour), it takes at most a couple of rain cells with very high intensity to overlap with each other. However, at timescales greater than this, it takes consecutive rainstorms to contain several rain cells with very high intensity, which happens with a low probability.

While the RBL model systematically underestimates the extreme rainfall at timescales of one day and more, the RBL-S2 model significantly eliminates this underestimation. The reason is as follows: First, note that the average inter-arrival time of rainstorms (λ^{-1}) ranges between 1.2 days and 2.7 days according to Table 1. Therefore, it is probable that time windows exceeding 1 day are likely to contain more than one rainstorm, so at this coarse timescale, the extreme rainfall depth is likely to be represented by more than a single storm. But the RBL model is less likely to have consecutive large rainstorms because the rainstorms are independent according to the model fundamental structure (See Section 2.2.1). On the contrary, the RBL-S2 model has an algorithm to induce the extreme rainstorms to gather together in the time series and fit in the time window yielding the extreme rainfall close to the observed one.

Figure 10 compares the past-168 hour (i.e. 7 days) rainfall of the annual maximum rainfall of the observed (x) and synthetic (y) rainfall. For convenience, we call this value the “P7 rainfall”. This value is important for the continuous hydrologic modelling studies in which antecedent moisture condition before the extreme events significantly influences the peak flow values. Several studies showed that the extreme rainfall does not always lead to the extreme flow discharge because of the varying antecedent soil moisture conditions (Briaud et al., 2009; Verhoest et al., 2010; Camici et al., 2011).

The RBL model systematically underestimated the P7 rainfall at the timescales between 5 minutes and 1 day. At the 3 day timescale, the value was well reproduced. The RBL-S2 model reduces the degree of underestimation of the P7 rainfall. This is also associated with the storm shuffling algorithm making similarly large storms gather together. It also suggests that the observed extreme rainfall events tend to occur during wet atmospheric and land surface conditions.

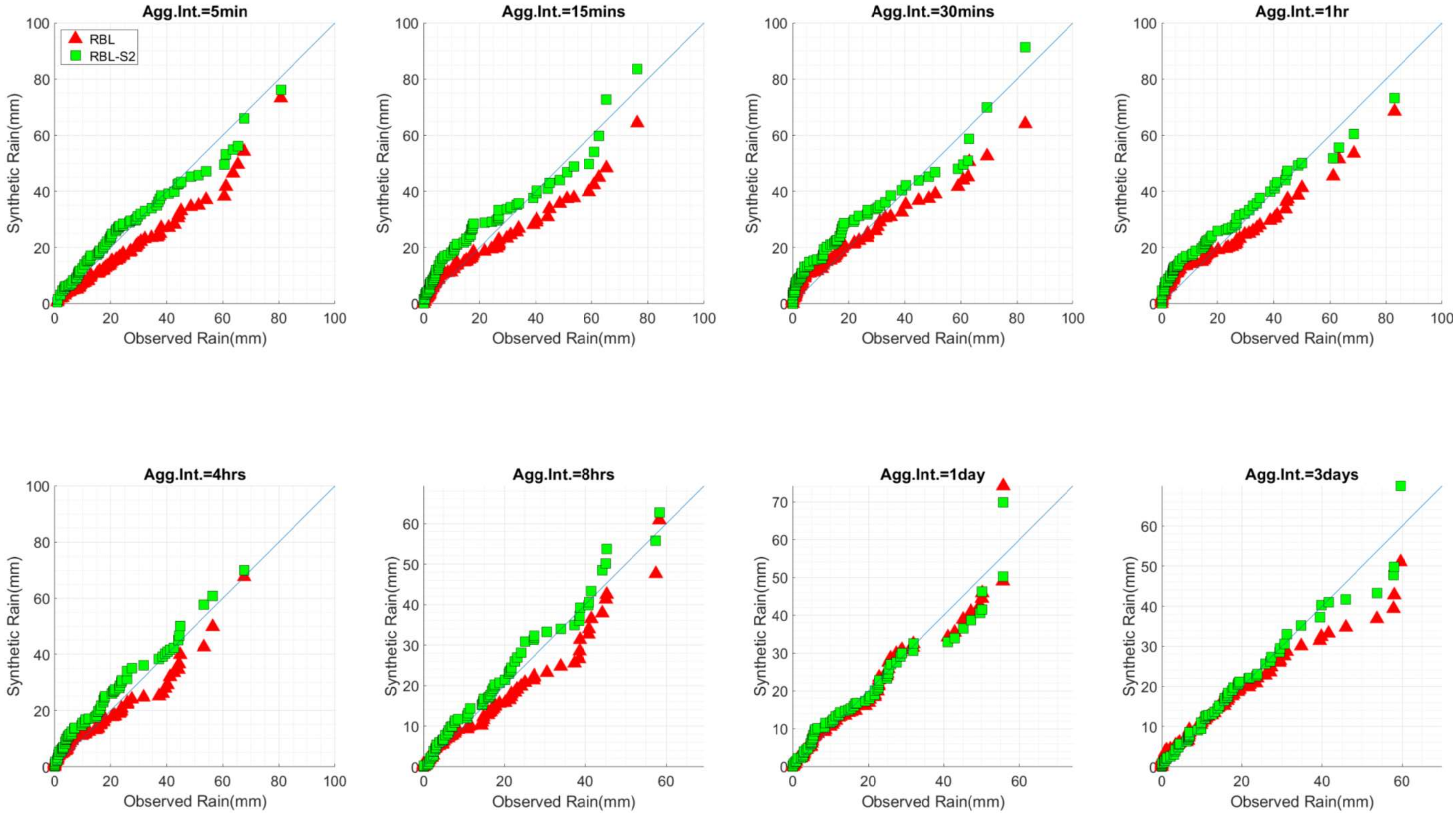

Figure 10. The Quantile-Quantile plot of the past-168hour (7days) rainfall of the annual maximum rainfall based on the RBL model and the RBL-S2 model.

4. Conclusion

Even though rainfall persistence or "memory" has been widely investigated (Koutsoyiannis, 2003; Ralph et al., 2006; Seneviratne et al., 2010; van der Ent and Savenije, 2011), its implications in practical applications have received relatively less attention. As Equation 1 suggests, the rainfall memory causes the large rainstorms to cluster together with large rainstorms and the small rainstorms with small rainstorms. This entails the occurrence of very large or small rainfall depths at coarser timescales which govern the design of the hydrologic system and hydraulic structures. Therefore, a good rainfall model must correctly reproduce the rainfall memory and the corresponding temporal correlation structure at a wide range of timescales.

This study proposed a stochastic rainfall model with algorithms designed to reflect the rainfall memory existing at different timescales. In this approach, first, a series of rainstorms are generated based on the traditional Poisson cluster rainfall model. Second, the generated rainstorms are rearranged so that rainstorms with similar depth cluster together. Third, this rainfall time series is rearranged again at the monthly timescale to reflect the rainfall correlation at timescales equal to and coarser than a month. The suggested model was validated using 69 years of 5-minute rainfall data observed at Bochum, Germany. The model successfully reproduced the mean, variance, correlation structure and skewness of rainfall depths, the proportion of wet/dry periods, as well as the extreme values at timescales from 5 minutes to a decade. On the other hand, the traditional Poisson cluster rainfall model performed well in terms of all these statistics simultaneously only for timescales not exceeding the inter-storm arrival time (approximately 1 to 3 days). The suggested model reproduced well the past-7-day rainfall before an extreme rainfall event that the traditional model systematically underestimated. The difference in the performance of the two models shows the importance of designing stochastic rainfall models to include rainfall memory at a large range of timescales.

The strength of the suggested model from a practical viewpoint is that it can be applied to provide the input rainfall data not only to a wide range of modelling studies addressing, for example, urban flood, landslides, and droughts but also to the studies assessing the compound impacts of the disasters simultaneously occurring at different timescales (Chen et al., 2011). We expect that the model will gather more attention as the hydrologic societies started to recognize the hydrologic, human, and environmental systems from a holistic viewpoint and interpreting them based on continuous and dynamic simulations (Wagener et al., 2010, Kim et al., 2018).

Software Kit

The software kit that implements the methodology of this study can be downloaded at the following website: http://www.letitrain.info/LetItRainDesktop.zip

Acknowledgement

This study was supported by the Basic Research Laboratory Program (NRF 2015-041523, 50 % grant) and the Basic Science Research Program (NRF 2018R1B5A2089503, 50% grant) through the NRF of Korea funded by the Ministry of Education.

Reference

Afifi, T., Milan, A., Etzold, B., Schraven, B., Rademacher-Schulz, C., Sakdapolrak, P., ... & Warner, K. (2016). Human mobility in response to rainfall variability: opportunities for migration as a successful adaptation strategy in eight case studies. Migration and Development, 5(2), 254-274.

Audet, C., & Dennis Jr, J. E. (2002). Analysis of generalized pattern searches. SIAM Journal on optimization, 13(3), 889-903.

Ayoub, A. T. (1999). Land degradation, rainfall variability and food production in the Sahelian zone of the Sudan. Land Degradation & Development, 10(5), 489-500.

Beecham, S., Rashid, M., & Chowdhury, R. K. (2014). Statistical downscaling of multi- site daily rainfall in a South Australian catchment using a Generalized Linear Model. International Journal of Climatology, 34(14), 3654-3670.

Berkelhammer, M., Sinha, A., Mudelsee, M., Cheng, H., Edwards, R. L., & Cannariato, K. (2010). Persistent multidecadal power of the Indian Summer Monsoon. Earth and Planetary Science Letters, 290(1-2), 166-172.

Bernardara, P., De Michele, C., & Rosso, R. (2007). A simple model of rain in time: An alternating renewal process of wet and dry states with a fractional (non-Gaussian) rain intensity. Atmospheric research, 84(4), 291-301.

Burton, A., Kilsby, C. G., Fowler, H. J., Cowpertwait, P. S. P., & O'connell, P. E. (2008). RainSim: A spatial–temporal stochastic rainfall modelling system. Environmental Modelling & Software, 23(12), 1356-1369.

Briaud, J. L., Govindasamy, A. V., Kim, D., Gardoni, P., & Olivera, F. (2009). Simplified method for estimating scour at bridges (No. FHWA/TX-09/0-5505-1). Texas. Dept. of Transportation. Research and Technology Implementation Office.

Camici, S., Tarpanelli, A., Brocca, L., Melone, F., & Moramarco, T. (2011). Design soil moisture estimation by comparing continuous and storm- based rainfall- runoff modeling. Water Resources Research, 47(5).

Carvalho, L. M., Jones, C., & Liebmann, B. (2004). The South Atlantic convergence zone: Intensity, form, persistence, and relationships with intraseasonal to interannual activity and extreme rainfall. Journal of Climate, 17(1), 88-108.

Chen, Y. S., Kuo, Y. S., Lai, W. C., Tsai, Y. J., Lee, S. P., Chen, K. T., & Shieh, C. L. (2011). Reflection of typhoon morakot—the challenge of compound disaster simulation. Journal of mountain science, 8(4), 571-581.

Chandler, R. E., & Wheater, H. S. (2002). Analysis of rainfall variability using generalized linear models: a case study from the west of Ireland. Water Resources Research, 38(10), 10-1.

Cho, H., Kim, D., Olivera, F., & Guikema, S. D. (2011). Enhanced speciation in particle swarm optimization for multi-modal problems. European Journal of Operational Research, 213(1), 15-23.

Coe, R., & Stern, R. D. (1982). Fitting models to daily rainfall data. Journal of Applied Meteorology, 21(7), 1024-1031.

Cowpertwait, P. S. (1991). Further developments of the Neyman- Scott clustered point process for modeling rainfall. Water Resources Research, 27(7), 1431-1438.

Cowpertwait, P., Isham, V., & Onof, C. (2007). Point process models of rainfall: developments for fine-scale structure. Proceedings of the Royal Society A: Mathematical, Physical and Engineering Sciences, 463(2086), 2569-2587.

Gommes, R., & Petrassi, F. (1996). Rainfall variability and drought in sub-Saharan Africa. SD dimensions, FAO.

Eltahir, E. A. (1998). A soil moisture–rainfall feedback mechanism: 1. Theory and observations. Water resources research, 34(4), 765-776.

Entekhabi, D., Rodriguez-Iturbe, I., & Castelli, F. (1996). Mutual interaction of soil moisture state and atmospheric processes. Journal of Hydrology, 184(1-2), 3-17.

Haan, C. T., Allen, D. M., & Street, J. O. (1976). A Markov chain model of daily rainfall. Water Resources Research, 12(3), 443-449.

Hawk, K. L., & Eagleson, P. S. (1992). Climatology of station storm rainfall in the continental United States: Parameters of the Bartlett-Lewis and Poisson rectangular pulses models.

Jesus, J., & Chandler, R. E. (2011). Estimating functions and the generalized method of moments. Interface focus, 1(6), 871-885.

Kaczmarska, J., Isham, V., & Onof, C. (2014). Point process models for fine-resolution rainfall. Hydrological Sciences Journal, 59(11), 1972-1991.

Kim, D., Olivera, F., Cho, H., & Socolofsky, S. A. (2013). Regionalization of the Modified Bartlett-Lewis Rectangular Pulse Stochastic Rainfall Model. Terrestrial, Atmospheric & Oceanic Sciences, 24(3).

Kim, D., Kwon, H. H., Lee, S. O., & Kim, S. (2016). Regionalization of the Modified Bartlett–Lewis rectangular pulse stochastic rainfall model across the Korean Peninsula. Journal of hydro-environment research, 11, 123-137.

Kim, D., Kwon, H., Giustolisi, O., & Savic, D. (2018). Current water challenges require holistic and global solutions. Journal of Hydroinformatics, 20(3), 533-534.

Kim, Y., & Wang, G. (2007). Impact of initial soil moisture anomalies on subsequent precipitation over North America in the coupled land–atmosphere model CAM3–CLM3. Journal of Hydrometeorology, 8(3), 513-533.

Koutsoyiannis, D., & Onof, C. (2001). Rainfall disaggregation using adjusting procedures on a Poisson cluster model. Journal of Hydrology, 246(1-4), 109-122.

Koutsoyiannis, D. (2003). Climate change, the Hurst phenomenon, and hydrological statistics. Hydrological Sciences Journal, 48(1), 3-24.

Kovats, R. S., Bouma, M. J., Hajat, S., Worrall, E., & Haines, A. (2003). El Niño and health. The Lancet, 362(9394), 1481-1489.

Kwon, H. H., Lall, U., & Obeysekera, J. (2009). Simulation of daily rainfall scenarios with interannual and multidecadal climate cycles for South Florida. Stochastic Environmental Research and Risk Assessment, 23(7), 879-896.

De Lima, M. I. P., & Grasman, J. (1999). Multifractal analysis of 15-min and daily rainfall from a semi-arid region in Portugal. Journal of hydrology, 220(1-2), 1-11.

Marani, M. (2005). Non‐ power‐ law‐ scale properties of rainfall in space and time. Water Resources Research, 41(8).Marshall, J. D., Shimada, B. W., & Jaffe, P. R. (2000). Effect of temporal variability in infiltration on contaminant transport in the unsaturated zone. Journal of contaminant hydrology, 46(1-2), 151-161.

Milan, A., & Ruano, S. (2014). Rainfall variability, food insecurity and migration in Cabricán, Guatemala. Climate and Development, 6(1), 61-68.

Mishra, A. and Desai, V.: Drought forecasting using stochastic models, Stoch. Env. Res. Risk A., 19, 326–339, 2005.

Modarres, R. and Ouarda, T. B.: Modeling the relationship between climate oscillations and drought by a multivariate GARCH model, Water Resour. Res., 50, 601–618, 2014.

Oh, M., Lee, D., Kwon, H., & Kim, D. (2016). Development of flood inundation area GIS database for Samsung-1 drainage sector, Seoul, Korea. Journal of Korea Water Resources Association, 49(12), 981-993.

Olsson, Jonas, and Paolo Burlando. "Reproduction of temporal scaling by a rectangular pulses rainfall model." Hydrological Processes 16.3 (2002): 611-630.

Onof, C. (2003). DEFRA Project: Improved methods for national spatial-temporal rainfall and evaporation modelling for BSM, Internal Report, No. 8, Mathematical expressions of generalized moments used in single-site rainfall models, December 16, 2003.

Onof, C., Chandler, R. E., Kakou, A., Northrop, P., Wheater, H. S., & Isham, V. (2000). Rainfall modelling using Poisson-cluster processes: a review of developments. Stochastic Environmental Research and Risk Assessment, 14(6), 384-411.

Onof, C., and Wheater, H. S. (1993). Modelling of British rainfall using a random parameter Bartlett-Lewis rectangular pulse model. Journal of Hydrology, 149(1-4), 67-95.

Onof, C. and Wang, L.-P.: Modelling rainfall with a Bartlett–Lewis process: New developments, Hydrol. Earth Syst. Sci. Discuss., https://doi.org/10.5194/hess-2019-406, in review, 2019.

Ralph, F. M., Neiman, P. J., Wick, G. A., Gutman, S. I., Dettinger, M. D., Cayan, D. R., & White, A. B. (2006). Flooding on California's Russian River: Role of atmospheric rivers. Geophysical Research Letters, 33(13).

Seneviratne, S. I., Corti, T., Davin, E. L., Hirschi, M., Jaeger, E. B., Lehner, I., ... & Teuling, A. J. (2010). Investigating soil moisture–climate interactions in a changing climate: A review. Earth-Science Reviews, 99(3-4), 125-161.

Singh, V. P. (1997). Effect of spatial and temporal variability in rainfall and watershed characteristics on stream flow hydrograph. Hydrological processes, 11(12), 1649-1669.

Singh, S. V., Kripalani, R. H., Shaha, P., Ismail, P. M. M., & Dahale, S. D. (1981). Persistence in daily and 5-day summer monsoon rainfall over India. Archives for meteorology, geophysics, and bioclimatology, Series A, 30(3), 261-277.

Van der Ent, R. J., & Savenije, H. H. G. (2011). Length and time scales of atmospheric moisture recycling. Atmospheric Chemistry and Physics, 11(5), 1853-1863.

Verhoest, N. E., Vandenberghe, S., Cabus, P., Onof, C., Meca- Figueras, T., & Jameleddine, S. (2010). Are stochastic point rainfall models able to preserve extreme flood statistics?. Hydrological processes, 24(23), 3439-3445.

Wagener, T., Sivapalan, M., Troch, P. A., McGlynn, B. L., Harman, C. J., Gupta, H. V., ... & Wilson, J. S. (2010). The future of hydrology: An evolving science for a changing world. Water Resources Research, 46(5).

Yoo, J., Kim, D., Kim, H., and Kim, T.: Application of copula functions to construct confidence intervals of bivariate drought frequency curve, J. Hydro-Environ. Res., 11, 113–122, 2016.